Information-Driven Path Planning for UAV With Limited Autonomy in Large-Scale Field Monitoring

Nicolas Bono Rossello, Renzo Fabrizio Carpio, *Graduate Student Member, IEEE*, Andrea Gasparri, *Senior Member, IEEE*, and Emanuele Garone

***Abstract*— This article presents a novel information-based mission planner for a drone tasked to monitor a spatially distributed dynamical phenomenon. For the sake of simplicity, the area to be monitored is discretized. The insight behind the proposed approach is that, due to the spatiotemporal dependencies of the observed phenomenon, one does not need to collect data on the entire area, which is one of the main limiting factors in unmanned aerial vehicle (UAV) applications due to their limited autonomy. In fact, unmeasured states can be estimated using an estimator, such as a Kalman filter. In this context, the planning problem becomes the one of generating a flight plan that maximizes the quality of the state estimation while satisfying the flight constraints (e.g., flight time). The first result of this article is the formulation of this problem as a special orienteering problem where the cost function is a measure of the quality of the estimation. This results in a mixed-integer semidefinite formulation, which can be optimally solved for small instances of the problem. For larger instances, a heuristic is proposed, which provides suboptimal results. Simulations numerically demonstrate the capabilities and efficiency of the proposed path-planning strategy. We believe that this approach has the potential to increase dramatically the area that a drone can monitor, thus increasing the number of applications where monitoring with drones can become economically convenient.**

***Note to Practitioners*—This article was motivated by the problem of performing large-scale field monitoring activities using unmanned aerial vehicle (UAV), which at the moment is very time-consuming and limits the definitive adoption of UAVs for this kind of activities. This problem is caused by the limited autonomy of commercial UAVs and the lack of systematic ways to plan missions so as to maximize the amount of information collected. This work starts from the observation that, in many applications, the phenomena that one wants to observe have dynamics and statistical properties. Accordingly, data that are not directly measured can be estimated with a characterizable observation error. In this article, we develop the theoretical foundations for an information-based path planning and define the problem of designing the optimal mission as an optimization problem based on the knowledge of the monitored phenomenon. The presented results have the potential to dramatically improve the effectiveness of drones for monitoring applications.**

***Index Terms*— Kalman filter, optimization, path planning, unmanned aerial vehicles (UAVs).**

I. Introduction

UNMANNED aerial vehicles (UAVs) are commonly used to perform field coverage activities. These vehicles are typically equipped with a large variety of sensors to take measurements of areas of interest. Applications for these kinds of systems include monitoring operations in agriculture [1], archeology [2], and civil infrastructures [3].

In many applications, remote sensing best practices use postprocessed information in the form of an orthomosaic [4]. An orthomosaic is essentially a geometrically corrected image obtained due to the composition of several overlapped photographs [5]. This technique implies an exhaustive and complete coverage of the area, commonly using boustrophedon patterns as the one shown in Fig. 1. However, in the case of precision farming or other monitoring domains, the creation of a complete orthomosaic can be extremely time-consuming and might require several flights to cover relatively small areas, thus limiting the real-world applicability of drones. To understand the dimension of the problem, it is worth to mention the experience of the H2020 EU project PANTHEON "Precision farming of hazelnut orchards" where the farming area consists of several hundreds of hectares, while the area that can be covered for each flight using a boustrophedon approach is less than half a hectare.

Given this common limitation in time and resources, the literature has focused on the definition of optimal policies that partially cover the area of interest. In this regard, many persistent monitoring works rely on graph-based strategies where the latency in between visits to every region is minimized [6]–[8]. However, these strategies consider a static and node-independent distribution of the phenomena, which makes them nonsuitable for physical systems with significant dynamics.

Manuscript received 12 August 2020; revised 9 March 2021; accepted 21 May 2021. Date of publication 14 June 2021; date of current version 5 July 2022. This article was recommended for publication by Associate Editor P. Tokekar and Editor C. Seatzu upon evaluation of the reviewers' comments. This work was supported by the European Commission (project PANTHEON—"Precision farming of hazelnut orchards") under Grant 774571. *(Corresponding author: Nicolas Bono Rossello.)*

Nicolas Bono Rossello is with the Service d'Automatique et d'Analyse des Systèmes, Université Libre de Bruxelles (ULB), 1050 Brussels, Belgium, and also with the Department of Engineering, Roma Tre University, 00146 Rome, Italy (e-mail: nbonoros@ulb.ac.be).

Renzo Fabrizio Carpio and Andrea Gasparri are with the Department of Engineering, Roma Tre University, 00146 Rome, Italy (e-mail: renzo.carpio@uniroma3.it; gasparri@inf.uniroma3.it).

Emanuele Garone is with the Service d'Automatique et d'Analyse des Systèmes, Université Libre de Bruxelles (ULB), 1050 Brussels, Belgium (e-mail: emgarone@ulb.ac.be).

Color versions of one or more figures in this article are available at https://doi.org/10.1109/TASE.2021.3085365.

Digital Object Identifier 10.1109/TASE.2021.3085365

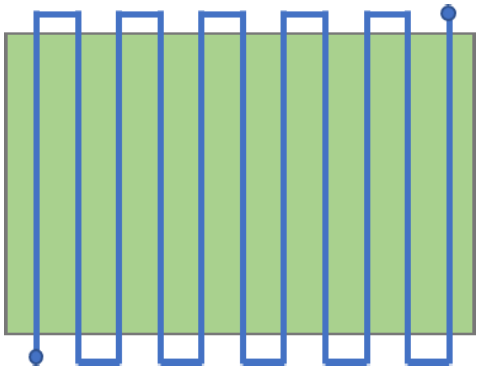

Fig. 1. Example of a boustrophedon pattern used for remote sensing.

Alternative approaches base their policies on the spatial correlation between the measurements. In these works, the mission path is computed so that it avoids redundant data and thus gathers the maximum amount of information per flight. In [9], UAVs equipped with omnidirectional sensors perform an information-based exploration where the goal is to minimize the time to obtain a predefined measure of data. In environment monitoring, the planning strategy is defined such that the measurement uncertainty of a Gaussian process (GP) regression is minimized [10], [11]. Also, in the field of autonomous underwater vehicles (AUVs), multiple AUVs are used to perform the sampling of a scalar field based on the information obtained [12]. These works optimize the path regarding the spatial distribution of the possible measurements. Yet, they tend to fail in the evaluation of the temporal correlation with previous data information, which is a meaningful aspect in most persistent monitoring activities.

In this article, we assume that the phenomena to be monitored have dynamics and statistical properties that are known. This is the case of, e.g., water distribution [13], [14] or dust deposition [15], [16]. We believe that a good monitoring policy must take advantage of these properties in the definition of the UAV path planning. In our work, we propose a path-planning strategy where the area of interest is only partially covered and the remaining elements are estimated based on the dynamics of the system and the spatial correlation between measurements. This approach resembles a sensor selection problem [17]–[19] where the measurement points are equivalent to the selection or not of available sensors in the observer formulation.

To the best of our knowledge, the literature presents only a few examples of path planning for spatiotemporal phenomena monitoring [20]–[22]. Binney *et al.* [20] defined a recursive greedy algorithm to compute waypoints based on a given indicator of the estimation process. For example, given a GP, the covariance of the estimation of different areas is minimized during a sensing exploration using AUVs. Garg and Ayanian [21] assumed a stochastic dynamic system and performed a multivehicle sampling where each robot moves such that the entropy of a particle filter is maximized. Lan and Schwager [22] modeled the phenomena as GPs and defined periodic trajectories to minimize the largest eigenvalue of the covariance of a Kalman Filter.

In this article, the path-planning policy is obtained as part of the estimation process of the monitored phenomena. This is achieved by structuring the path planning as an orienteering problem (OP) [23]. The OP is a combinatorial problem that consists of a node selection where the shortest path in between the selected nodes is determined. Given a time or length constraint, the objective is to maximize the score given by the visited points. We believe that UAV remote sensing activities, due to the flight time restriction and the discrete nature of the measurements, are naturally recast in OPs. In this context, the set of points represents the possible measurement coordinates, the time interval is adapted to the vehicle autonomy, and the cost function is some measure related to the measurement points.

Some works in path planning already propose tentative information-based policies based on the OP. In [24], the information obtained is maximized using a quadratic utility function to represent the spatial relation between the different measurement points. More recently, Bottarelli *et al.* [25] introduced an orienteering-based path planning used to optimize a level set estimation. In such work, the measurement points are selected such that the accuracy of the level sets classification is maximized.

The main contribution of this article is the definition of the OP based on the maximization of the Fisher information matrix of a Kalman filter with intermittent observations to monitor a dynamic phenomenon. The main advantage of this approach is that the path of the UAV is computed considering the process dynamics, the estimation uncertainty and the existing fixed sensing structure. By doing so, it allows to define the optimal combination of the UAV remote sensing with additional sensing devices by resorting to an observer-based architecture.

This work focuses on the case where the monitored phenomena can be modeled as linear time-invariant systems subject to Gaussian noise, a common assumption in field monitoring of physical phenomena [26]–[28]. Also, we assume that the monitoring is performed by a UAV with a flight time that is much shorter than the time constants of the monitored system.

The developed strategy provides an offline computation of the optimal sensing areas over one step ahead horizon of the estimation process. This approach allows obtaining the optimal path in cases where the coverage is done with unknown periodicity or when the time gap between flights is large.

In order to solve this problem we propose a mixed-integer semidefinite programming (MISDP) formulation where the minimum eigenvalue of the information matrix is maximized. This formulation allows to obtain the optimal solution for small instances of the problem. In addition, for the case of large-scale scenarios, a heuristic is proposed along with an exhaustive computational analysis.

The remainder of this article is organized as follows. In Section II, the problem is stated and defined. Section III provides the proposed estimation measure to monitor the phenomena and Section IV introduces the problem formulation for the information-based path planning. In Section V, a heuristic strategy is introduced, and in Section VI, simulations are performed to compare the performance of the proposed method

with traditional strategies. In Section VII, conclusions and future work directions are discussed.

II. Problem Setting

Consider a plane partitioned in N areas and let the linear time-invariant system

$$x_{k+1} = Ax_k + Bu_k + w_k \tag{1}$$

describe the dynamic phenomenon that we want to observe. We assume that the state vector is in the form

$$x_k = \begin{bmatrix} x_k^1 \\ \dots \\ x_k^N \end{bmatrix}$$

where $x_k^i \in \mathbb{R}^n$ represents the states of the system at time k in the ith area and $u_k \in \mathbb{R}^n$ is the vector of the (measured) inputs to the system at that time instant. The complete state vector is thus $x_k \in \mathbb{R}^{Nn}$ and the matrices are $A \in \mathbb{R}^{Nn \times Nn}$ and $B \in \mathbb{R}^{Nn \times n}$. The system is subject to a process disturbance $w_k \backsim N(0, Q)$ modeled as a stochastic Gaussian noise with covariance $Q \in \mathbb{R}^{nN \times nN}$, which is typically nondiagonal and has nonzero terms for variables describing adjacent areas.

To estimate the state of this process, two classes of sensors are assumed available: fixed sensors and a mobile sensor. An example of this configuration can be found in water stress monitoring for precision agriculture, which typically combines fixed soil moisture sensors and periodical sensing flights carried out by UAVs.

We denote with $C_i \in \mathbb{R}^{M^i \times n}$ the measurement matrix associated with the measurements that can be potentially performed on the ith area. This matrix consists of two submatrices

$$C_i = \begin{bmatrix} C_i^f \\ C_i^m \end{bmatrix} \quad \forall i = 1, \dots, N \tag{2}$$

where $C_i^f \in \mathbb{R}^{f_i \times n}$ denotes the available fixed measurements of the ith area and $C_i^m \in \mathbb{R}^{m_i \times n}$ is the matrix associated with the outputs that can be measured if the area is visited by a mobile sensor.

The combination of the measurement matrices of each area provides a time-invariant observation matrix $C \in \mathbb{R}^{M \times Nn}$, where M is the total number of measurable states, in the form of a block-diagonal matrix

$$C = \begin{bmatrix} C_1 & \dots & O_{M^1 \times n} \\ \vdots & \ddots & \vdots \\ O_{M^N \times n} & \dots & C_N \end{bmatrix} \tag{3}$$

which defines the information of the system that can be accessed to through the two classes of sensors, with M^i the number of states that can be retrieved from the ith area.

To represent the fact that at a time instant k, an area might or might not be visited by the UAV, and we introduce the binary variable γ_k^i. In particular, $\gamma_k^i = 1$ if the ith area is visited at time k, and $\gamma_k^i = 0$ otherwise. Accordingly, we define the measurement selection matrix Γ_k^i corresponding to each area as

$$\Gamma_k^i = \begin{bmatrix} I_{f_i \times f_i} & O_{f_i \times m_i} \\ O_{m_{i,k} \times f_i} & I_{m_{i,k} \times m_{i,k}} \end{bmatrix} \tag{4}$$

where $m_{i,k} = \gamma_k^i m_i$. In other words

$$\Gamma_k^i = \begin{cases} \begin{bmatrix} I_{f_i \times f_i} & O_{f_i \times m_i} \\ O_{m_i \times f_i} & I_{m_i \times m_i} \end{bmatrix}, & \text{if } \gamma_k^i = 1 \\ [I_{f_i \times f_i} \quad O_{f_i \times m_i}], & \text{if } \gamma_k^i = 0. \end{cases} \tag{5}$$

Accordingly, the selection of the available measurements at time k is provided by the matrix $\Gamma_k \in \mathbb{R}^{M_k \times M}$, which is computed as

$$\Gamma_k = \Gamma_k^1 \oplus \Gamma_k^2 \oplus \dots \oplus \Gamma_k^N = \begin{bmatrix} \Gamma_k^1 & \dots & O_{M^1 \times n} \\ \vdots & \ddots & \vdots \\ O_{M^N \times n} & \dots & \Gamma_k^N \end{bmatrix} \tag{6}$$

where $\oplus$ denotes the direct sum operator and M_k represents the number of measurements available at time k.

Using this matrix, we can write the measurement equation of the entire system as

$$y_k = \Gamma_k(Cx_k + v_k) \tag{7}$$

where $y_k \in \mathbb{R}^{M_k}$ is the set of measurements available to the system at time k and v_k represents the measurement noise, which is assumed to be stochastic Gaussian noise $v_k \backsim N(0, R)$ with diagonal covariance matrix $R \in \mathbb{R}^{M \times M}$.

Due to autonomy limitations, at each sampling time, the UAV can collect information only on a limited amount of areas. To model this, in this article, we will consider the following reasonable assumptions concerning the mobile sensor.

1) The visit of an area is equivalent to the visit of its centroid.
2) At each time k, the mobile sensor has a limited maximum autonomy $T_{\max,k} > 0$ (e.g., in the case of a UAV this is the flight time).
3) Let the time step of the linear system be Δt, the maximum autonomy of the mobile sensor is considerably smaller, i.e., $T_{\max,k} \ll \Delta t \ \forall k \in \mathbb{R}$.
4) The budget of autonomy that is spent to go from the centroid of the area i to the centroid of the area j is a fixed quantity t_{ij} (in the case of a UAV the time to travel from i to j).

Accordingly, we can define the UAV trajectory as a path on an undirected and connected graph $G =< V, E >$, where $V = \{0, 1, 2, \dots, N, N+1\}$ and $E \subset V \times V$ are the set of vertices and arcs, respectively.

The vertices $1, \dots, N$ represent the labels of the centroids of each area, whereas the vertices 0 and $N+1$ represent predefined starting and ending positions for each mission (in the case of a UAV are the takeoff and the landing pads, which usually coincide).

Concerning the edges, in line of principle, any set of arcs that makes the graph E connected can be selected. In this article, without any loss of generality, we will focus on the realistic case that $(0, j) \in E, (j, N+1) \in E, \forall j = 1, \dots, N$ and that an edge (i, j) with $i, j \in \{1, \dots, N\}$ exists only if the ith area and the jth area are adjacent. This allows the remote sensing activity to start from the most convenient area i and not to be constrained by the position of the takeoff and

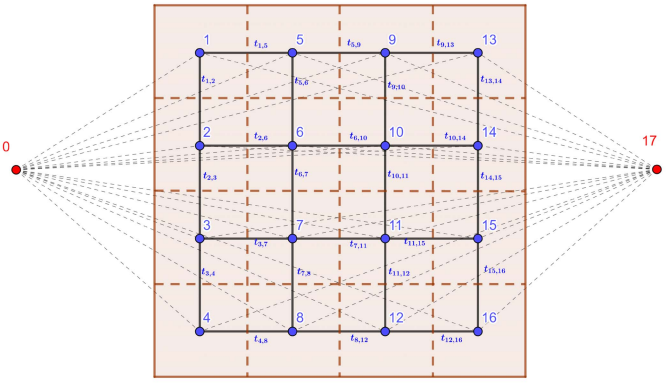

Fig. 2. Example of the regular grid obtained for a monitored area.

landing pads. This assumption also considers that in several remote sensing applications, the speed during the sensing must be lower than during the takeoff and the landing. Each edge $(i, j) \in E$ has an associated weight t_{ij} representing the amount of autonomy spent to travel from vertex i to vertex j. The overall graph is shown in Fig. 2.

We reiterate that the final and initial points 0 and $N+1$ do not need to coincide, but they may represent the same physical point depending on the application.

The goal of this article is to compute at each sampling time k a feasible path for the UAV so that some measure of the information collected is maximized given the limited autonomy of the vehicle. In other words, this article aims at solving the following problem.

Problem 1: Determine the optimal ordered sequence of nodes

$$S_k = [s_1, s_2, \ldots, s_{n_k}] \tag{8}$$

which solves the following optimization problem:

$$\arg\max_{S_k} f(S_k) \tag{9}$$

$$\text{s.t. } s_1 = 0 \tag{10}$$

$$s_{n_k} = N + 1 \tag{11}$$

$$(s_i, s_{i+1}) \in E, \quad i = 0, \ldots, n_k - 1 \tag{12}$$

$$\sum_{i=1}^{n_k-1} t_{s_i, s_{i+1}} \leq T_{\max,k} \tag{13}$$

where $f(\cdot)$ is a suitable measure of the quality of the collected information. In Section III, we will characterize this measure of the information to be maximized.

III. Estimation of the Monitored System

Since system (1) is a linear system subject to Gaussian noise and given the occasional availability of mobile sensing, the most natural choice to estimate the state is the Kalman filter with intermittent observations (see [29], [30]). This choice is based on the fact that the Kalman filter is the optimal estimator with respect to any quadratic function of the estimation in the case of linear systems subject to white noise [31].

The prediction step of this estimator is

$$\hat{x}_{k|k-1} = A\hat{x}_{k-1|k-1} + Bu_k \tag{14}$$

$$P_{k|k-1} = AP_{k-1|k-1}A^T + Q \tag{15}$$

and the correction step is

$$\hat{x}_{k|k} = \hat{x}_{k|k-1} + K_k(y_k - C_k\hat{x}_{k|k-1}) \tag{16}$$

$$K_k = P_{k|k}C_k^T(C_kP_{k|k-1}C_k^T + R_k)^{-1} \tag{17}$$

$$P_{k|k} = P_{k|k-1} - K_kC_kP_{k|k-1} \tag{18}$$

where $\hat{x}_{k|k}$ is the estimated value of the state at time k given the information available at that time and $P_{k|k}$ is the error covariance matrix of the estimation. The time-varying matrices C_k and R_k are defined as $C_k = \Gamma_k C$ and $R_k = \Gamma_k R \Gamma_k^T$, respectively.

The quality of the state estimation process after the kth data collection is typically based on the error covariance matrix $P_{k|k}$. Combining (17) and (18) and applying the matrix inversion lemma, this matrix can be expressed as

$$P_{k|k} = \left[P_{k|k-1}^{-1} + C_k^T R_k^{-1} C_k\right]^{-1}. \tag{19}$$

The main issue of using some function of the covariance matrix as a cost function is that, because of the inversion, this is a nonlinear function of the decision variables γ_k^i.

An alternative to the covariance matrix is the Fisher information matrix Y_k. This matrix describes the quantity of information associated with each variable and, for the case of a linear system, is equivalent to $Y_{k|k} = P_{k|k}^{-1}$ [32]. Accordingly, the postinformation matrix of the estimator can be expressed as

$$Y_{k|k} = P_{k|k-1}^{-1} + C_k^T R_k^{-1} C_k \tag{20}$$

which provides a simpler expression. Since in this article the matrix $R_k \in \mathbb{R}^{M_k \times M_k}$ is assumed to be a diagonal matrix, the Fisher information matrix (20) can be simplified as

$$Y_{k|k} = P_{k|k-1}^{-1} + \sum_{i}^{M_k} \frac{C_{k,i}^T C_{k,i}}{r_{k,i}} \tag{21}$$

where $r_{k,i}$ is the ith diagonal entry of the matrix R_k and $C_{k,i}$ is the observation matrix when only the measurement of the ith entry is available. We can further simplify the expression by separating the contribution from mobile and fixed sensors as

$$Y_{k|k} = P_{k|k-1}^{-1} + \sum_{i=1}^{N} C_{f,i}^T \left(R_i^f\right)^{-1} C_{f,i} + \sum_{i=1}^{N} \gamma_{i,k} \left(C_{m,i}^T \left(R_i^m\right)^{-1} C_{m,i}\right) \tag{22}$$

where $C_{f,i}$ represents the observation matrix C whose only nonzeros entries belong to the fixed measurements of the area i and, similarly, $C_{m,j}$ denotes the matrix C with entries associated with the UAV measurements. In this reformulation, the information matrix is conveniently defined as a linear function of the binary variable γ_k^i.

When working with covariance matrices, a common measure of performance is the trace of the covariance matrix. However, in the case of the Fisher information matrix, it has been shown [33] that its trace does not distinguish the gains based on the value of the eigenvalues. Therefore, the trace fails to provide an appropriate measurement of the information.

In this article, we propose as a performance objective the maximization of the minimum eigenvalue of the Fisher

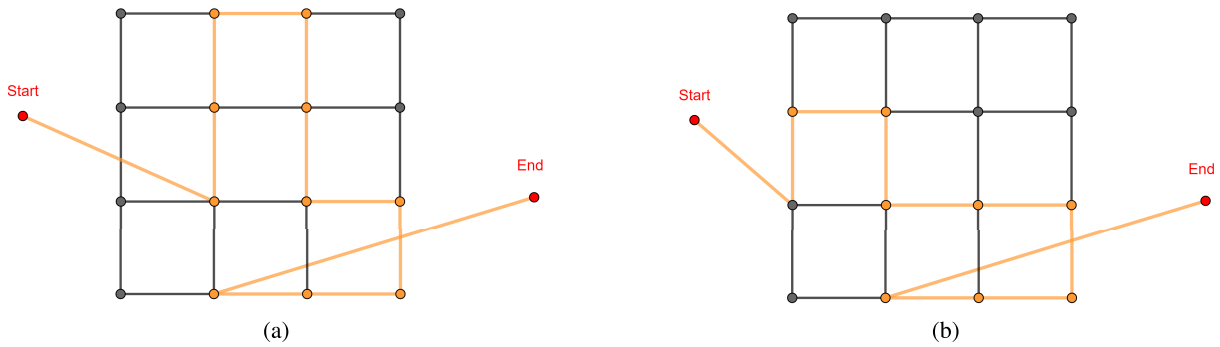

Fig. 3. Examples of feasible paths. (a) Generated path 1. (b) Generated path 2.

information matrix. The use of the minimum eigenvalue is another way to define a *measure* of a matrix (see [34]) that penalizes the uncertainty in the states with the lowest Fisher information. This approach has been shown to provide a good measure of the overall uncertainty in the estimation of parameters [35], [36].

The performance objective can be synthetically described as

$$\max_{\alpha,\gamma_k^i} \quad \alpha$$
$$\text{s.t. } P_{k|k-1}^{-1} + \sum_{i=1}^{N} C_{f,i}^T \left(R_i^f\right)^{-1} C_{f,i} + \sum_{i=1}^{N} \gamma_{i,k} \left(C_{m,i}^T \left(R_i^m\right)^{-1} C_{m,i}\right) \geq \alpha I. \tag{23}$$

In this setting, the problem becomes the one of determining at each time a sequence of nodes S_k satisfying (8)–(13) that maximizes (23), where $\gamma_{i,k} = 1$ if and only if $i \in S_k$.

It is very important to remark that, due to the statistical properties of the linear Kalman filter, the covariance, the information matrix, and any metric associated with it do not depend on the actual values of the measurements but only on the covariance at time $k-1$ and of the sensing structure $\Gamma_k C$ used at time k.

IV. Information-Based OP

The problem described in Sections II and III can be seen as a special OP where we have to select a subset of nodes to be visited and their order so that the information is maximized and the autonomy constraints are satisfied.

In this section, following an approach inspired by the Miller–Tucker–Zemlin (MTZ) formulation of the TSP [37], we will propose a convenient mathematical formulation of this particular OP. To this end, let us introduce two sets of decision variables: 1) the binary variable q_{ij} whose value is 1 if the node j is visited after the node i and 0 otherwise and 2) the integer variable u_i which denotes the visiting order of the node i.

The choice of an initial and final point is enforced by the following constraints:

$$\sum_{i=1}^{N} q_{0i} = \sum_{j=1}^{N} q_{jN+1} = 1 \tag{24}$$

$$\sum_{i=1}^{N} q_{i0} = \sum_{j=1}^{N} q_{N+1j} = 0. \tag{25}$$

For the rest of the nodes, we must ensure that each node is visited at most once and the continuity on the sequence of edges selected

$$\sum_{i \in N_p} q_{ip} = \sum_{j \in N_p} q_{pj} \leq 1; \quad \forall p = 1, \ldots, N \tag{26}$$

where $N_p = \{i | (i, p) \in E\}$ denotes the set of neighbors of the node $p \in V$. The endurance constraints are formalized as

$$\sum_{i=1}^{N-1} \sum_{j \in N_i} t_{ij} q_{ij} \leq T_{\max,k}. \tag{27}$$

To avoid possible subtours and to ensure the continuity of the path, it must hold that

$$2 \leq u_i \leq N \quad \forall i = 1, \ldots, N, \tag{28}$$

$$u_i - u_j + 1 \leq (N-1)(1 - q_{ij}) \quad \forall i, j = 2, \ldots, N, \ (i, j) \in E. \tag{29}$$

Constraints (24)–(29) ensure the feasibility of the UAV path. Fig. 3 shows two examples of feasible and continuous paths.

Note that the fact of sensing the ith area at time k, previously introduced as $\gamma_{i,k} = 1$, is equivalent to the condition $\sum_{j \in N_i} q_{ji} = 1$. Therefore, combining the path-planning integer constraints (24)–(29) with (23), where we substitute $\gamma_{i,k} = \sum_{j \in N_i} q_{ji}$, the following optimization problem is obtained:

$$\max_{\alpha,q,u} \quad \alpha$$
$$\text{s.t. } P_{k|k-1}^{-1} + \sum_{i=1}^{N} C_{f,i}^T \left(R_i^f\right)^{-1} C_{f,i} + \sum_{i=1}^{N} \sum_{j \in N_i} q_{ji} \left(C_{m,i}^T \left(R_i^m\right)^{-1} C_{m,i}\right) \geq \alpha I$$
$$\sum_{i=1}^{N} q_{0i} = \sum_{j=1}^{N} q_{jN+1} = 1$$
$$\sum_{i=1}^{N} q_{i0} = \sum_{j=1}^{N} q_{N+1j} = 0$$
$$\sum_{i \in N_p} q_{ip} = \sum_{J \in N_p} q_{pj} \leq 1; \quad \forall p = 1, \ldots, N$$
$$\sum_{i=1}^{N-1} \sum_{j \in N_i} t_{ij} q_{ij} \leq T_{\max,k}$$

$$
\begin{aligned}
&2 \le u_i \le N \quad \forall i = 1, \ldots, N \\
&u_i - u_j + 1 \le (N-1)(1 - q_{ij}) \\
&\quad \forall i, j = 1, \ldots, N+1, (i, j), \in E \\
&q_{ij} \in \{0, 1\} \quad \forall i, j = 0, \ldots, N+1, \ (i, j) \in E. \quad (30)
\end{aligned}
$$

In this formulation, the information-based path planning is expressed as an MISDP problem, which, for reasonably small instances of the problem, can be solved optimally using commercial solvers such as *SCIP* or *cutsdp* [38], [39]. Nevertheless, it remains an NP-hard problem whose solving time grows excessively in the case of large instances of the problem.

V. Proposed Heuristic

In this section, we propose a heuristic to compute a suboptimal path based on the integer relaxation of the mixed-integer problem (30). The goal is to obtain a close-to-optimal algorithm that can be used in large-scale scenarios.

Note that the optimization problem (30) becomes a convex problem when the integer variables $q_{i,j}$ and u_i are relaxed. Consider $q_{i,j} \in [0, 1]$ and $u_i \in \mathbb{R}$, such that both variables can take real values, and then, Problem (30) is reformulated as a semidefinite programming (SDP) problem, which can be effectively and quickly solved by SDP solvers, such as *Mosek* [40].

The outcome of this convex problem, q_{ij}^r, provides the values between 0 and 1 for the edges (see Fig. 4), which can be seen as how likely is the edge (i, j) to be taken in the optimal path. Therefore, a suboptimal solution can be obtained by computing heuristics, which selects the points to visit based on these values [41].

Algorithm 1 selects the path by rounding up each link (i, j) with probability q_{ij}^r. The algorithm starts by the initial point and sequentially adds nodes to the path based on the edges that are rounded up to 1. In this case, for each selected point i, there exists a set $Q_i^r = \cup_{j \in N_i} q_{ij}^r$ where each element represents the probability of choosing an adjacent edge j such that $\sum_{j \in N_i} q_{ij}^r = 1$. This step can be seen as a fitness proportionate selection problem where the next edge is probabilistically chosen based on the solution of the relaxed problem. This selection can be done by using a roulette selection method or other selection-based methods [42], [43].

To ensure that the obtained path is feasible and continuous, the rounding is done sequentially based on the previous edge selected. The algorithm starts from the initial point V_{ini} adding edges until the maximum flight time $T_{\max}$ is reached. This process is shown in Fig. 5.

To converge to a close-to-optimal solution, the operation is repeated for a sufficiently large number of L iterations, which is tuned numerically. After each iteration, the minimum eigenvalue associated with the computed path, $\lambda_1(X_{\text{path}})$, is compared with the previously stored solution. If the new path improves the currently stored sequence, the latter is replaced and the algorithm keeps seeking for alternative paths. By doing so, the computational cost is proportional to the autonomy of the vehicle (number of nodes that can be visited in one flight) and the number of iterations L, keeping a constant computational complexity in the rounding selection regardless of the size of the area.

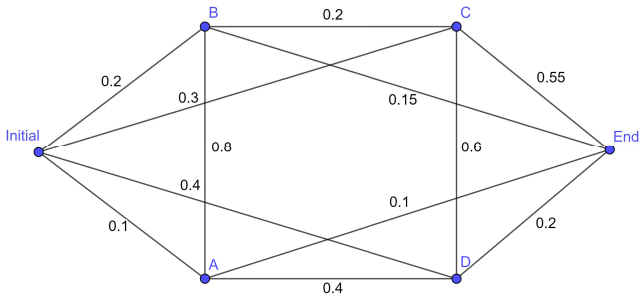

Fig. 4. Example of a possible solution of the relaxed problem.

Algorithm 1 Sequentially Edge Randomized Rounding

Input: Solution G_{rel}
Output: Set of edges X_{path} where $\lambda_1(X_{path})$ is maximized

$X_{path} \leftarrow \emptyset$
for $it \le L$ **do**
  $X_{temp} \leftarrow \emptyset$
  $X_{new} \leftarrow \emptyset$
  $i \leftarrow 0$ % Start from initial node 0
  while $(T(X_{temp}) + t_{i,N+1} \le T_{max})$ **do**
    Select q_{ij} given $(i, j) \in E$ by randomized rounding
    $X_{new} \leftarrow q_{ij}$
    if $T(X_{new}) + t_{i,N+1} \le T_{max})$ **then**
      $i \leftarrow j$ % Move to next node j
      $X_{temp} \leftarrow q_{ij}$
    else
      BREAK
    end if
  end while
  $X_{temp} \leftarrow q_{iN+1}$
  if $\lambda_1(X_{temp}) \ge \lambda_1(X_{path})$ **then**
    $X_{path} \leftarrow X_{temp}$
  end if
end for
Output X_{path}

VI. Simulation Results and Application

This section provides, through numerical simulations, an illustration of the effectiveness of the information-based path planning introduced in this article. To do so, the adaptability of the path, the evolution over time, and the performance are analyzed and compared against a traditional covering strategy.

To provide a more constructive visualization, the simulations are based on a realistic precision agriculture scenario.

A. Case Study: Precision Agriculture

The effectiveness of the proposed planning method is shown through a numerical example. In this example, inspired by the H2020 EU project PANTHEON "Precision farming of hazelnut orchards," we consider a hazelnut orchard where we

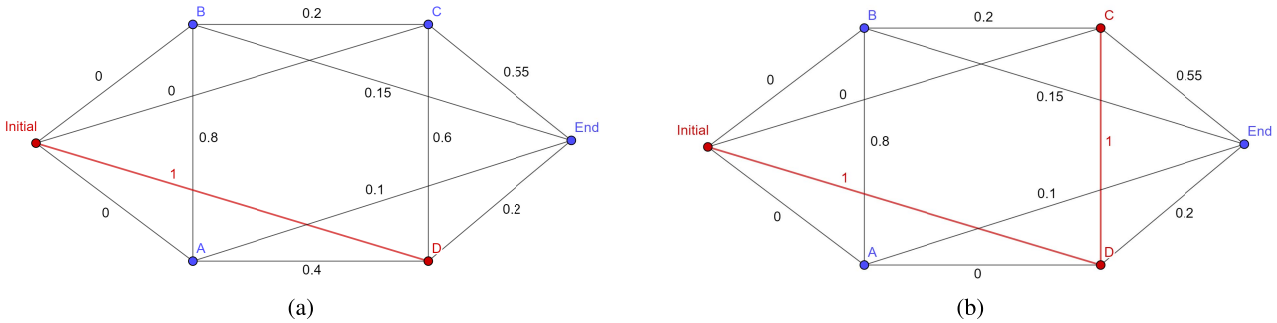

Fig. 5. One step of the randomized rounding algorithm. (a) Step 1. (b) Step 2.

want to estimate the water content of the plants and soil using the information collected by a drone and an agrometeorological IoT network composed of a network of fixed soil humidity sensors distributed in the orchard and a weather station providing some climate and rainfall measurements in real time.

In particular, we consider an orchard of p plants and N soil parcels, which can be described by a linear system in the form

$$\begin{cases} x_{k+1} = Ax_k + Bu_k + B_d\hat{d}_k + w_k \\ y_k = \Gamma_k(Cx_k + v_k) \end{cases} \tag{31}$$

where $x = [x_1^T \ x_2^T \ x_3^T]^T \in \mathbb{R}^{N+2p}$ is the state vector with $x_1 = [\theta_1, \ldots, \theta_N]^T$ the soil moisture status, $x_2 = [W_1, \ldots, W_p]^T$ the water plant status, and $x_3 = [W_{\text{rem},1}, \ldots, W_{\text{rem},p}]^T$ the water status of the leaves. u_k represents the irrigation inputs and $\hat{d}_k$ represents the meteorological disturbances. The used system dynamics mimic the experimental setting proposed in the PANTHEON project, which comprises a portion of an orchard within the "Azienda Agricola Vignola," a farm located in the province of Viterbo, Italy. The model and the parameters used to describe the water dynamics are the ones presented in [44]. In this model, it is assumed that the fixed sensors are able to capture the value of soil moisture in the area where they are deployed and that the drone is able to measure the water status of the leaves. For further information about the model, the reader is referred to [44].

B. Computational Analysis of the Heuristic

This section presents a study of the scalability, accuracy, and computational performance of the presented heuristic with respect to the optimal formulation (30).

Simulations are performed given different size areas, ranging from grids of 4×4 up to 6×6 nodes. In order to obtain meaningful results, for each problem size, 100 simulations have been performed varying the information distribution of the process. For this test, the autonomy of the vehicle is such that it allows to visit a maximum of 6 to 9 nodes depending on the size of the grid.

Table I shows the average level of degradation provided by these simulations from the heuristic with respect to the optimal values. This degradation is computed as

$$\triangle = \left(1 - \frac{\lambda_1(\text{heuristic})}{\lambda_1(\text{optimal})}\right) * 100. \tag{32}$$

TABLE I

SOLUTION DEGRADATION BETWEEN THE PROPOSED STRATEGY AND THE OPTIMAL STRATEGY

Grid size	Degradation ($\triangle$)
4×4	4.80%
5×5	3.82%
5×6	3.46%

TABLE II

COMPARISON COMPUTATIONAL TIME BETWEEN THE OPTIMAL AND THE PROPOSED STRATEGY

Path planner	Computational time (s)			
	4×4	5×5	5×6	6×6
Algorithm 1	1.96	1.91	2.20	2.24
Optimal	8.12	169.06	372.58	> 3600

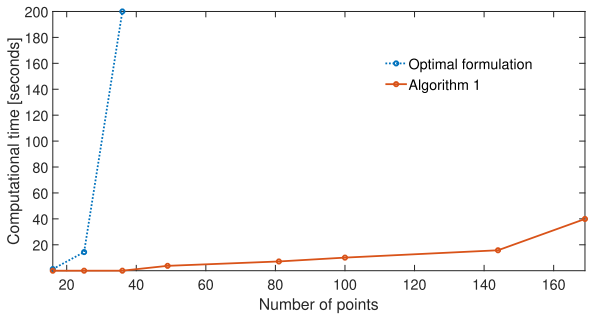

Fig. 6. Evolution of the computational time for the different methods.

As reported in Table II, the heuristic is able to obtain results with less than 5% of degradation with respect to the optimal solution while requiring a much lower computational time.

Table II shows the average time used to obtain the solution to the path-planning problem. In this case, for more than 36 nodes (a grid of 6×6), we can observe how the computational time for the mixed-integer formulation of the problem becomes prohibitive. On the contrary, the heuristic strategy, as shown in Fig. 6, always provides reasonable computational times.

C. Simulations

In this section, the performance of the path planning is illustrated. Simulations are carried out for two different distributions of the ground sensors. The two scenarios are shown

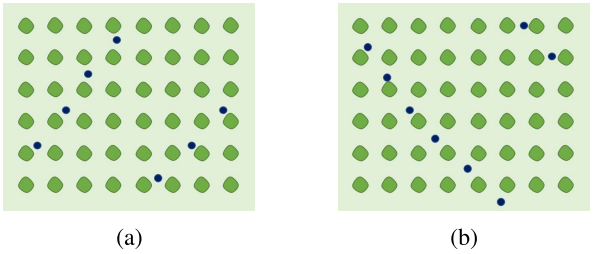

(a) (b)

Fig. 7. Fixed sensor distributions. (a) Distribution 1. (b) Distribution 2.

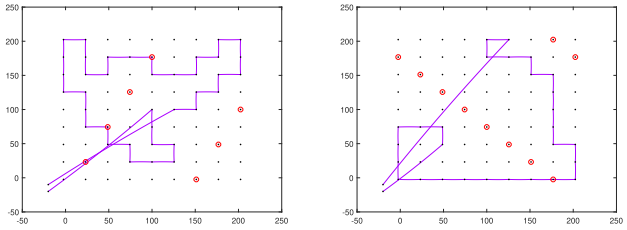

(a) (b)

Fig. 8. Comparison of the obtained path according to the soil sensor distribution. (a) Path for distribution 1. (b) Path for distribution 2.

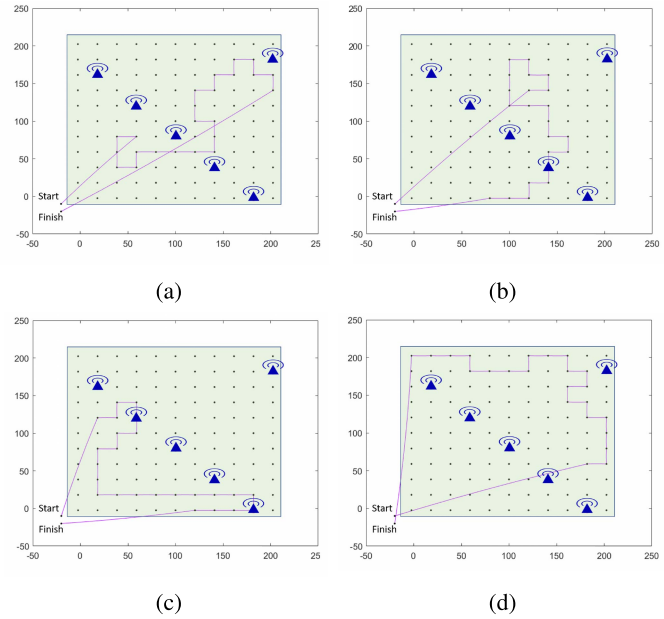

(a) (b) (c) (d)

Fig. 9. Iterative path evolution. (a) Flight 1. (b) Flight 2. (c) Flight 3. (d) Flight 4.

in Fig. 7. Note that the areas close to the fixed sensors have more information about the water states than the more isolated areas. Therefore, one can expect that changing the location of the sensors the information distribution changes too [17] and, thus, the optimal covering path.

The paths obtained for both distributions are shown in Fig. 8. These results show how the optimal path changes according to the fixed sensor position. It must be noted that the paths are evaluated with respect to the information obtained and that the total path time is a constraint of the problem. Thus, postprocess reordering of the points obtained (based on TSP methods) could improve the heuristic solution in the case it allows the visit of additional points, increasing the information collected. If the reordering does not allow to visit any additional point, as it is the case of flight from Fig. 8(a), there might exist several feasible and optimal paths that visit the same areas in different order within the time limit.

Clearly, the path strongly depends on the information distribution available before the measurement. To highlight this, a small area of an orchard has been simulated and four sampling periods considered. The resulting paths are shown in Fig. 9. As it can be seen from the four plots, the areas with less information change accordingly to the already covered points and so does the path, demonstrating the spatial and temporal awareness of the presented strategy.

D. Performance Analysis

In this section, an iterative implementation of the presented path-planning strategy is compared against a very common persistent monitoring strategy based on field partitioning, where the area is divided into an equal number of partitions coherent with the flight autonomy and the partitions are covered sequentially [45], [46]. In this case, given the symmetry of the graph and the area considered, the maximum number of points that can be visited at each flight is equal to the number of points of each partition. This fact implies that there is no sequence of flights that provides a lower latency between visits to each node. This allows comparing our strategy against a policy based only on visiting latency, another commonly used indicator in permanent monitoring [6], [7].

To make a fair comparison, the maximum flight time obtained for the partition strategy is common for all the sensing strategies. The model is simulated over a horizon of 350 h. The data used for the meteorological disturbances come from the measurements of the PANTHEON weather station in the Azienda Agricola Vignola in the area of Viterbo (Italy). The flights are performed with a nonuniform sampling period ranging between 35 and 70 h, to realistically simulate logistics and weather uncertainty.

First, to compare also with the optimal strategy proposed in Section IV, a simulation for a small grid of 6×6 nodes is performed. In Fig. 10, the evolution of the minimum eigenvalue of the information matrix is shown. In this figure, the partitioning strategy is referred to as *arbitrary division* and *heuristic strategy*, which corresponds to Algorithm 1. From this plot, it can be seen that the presented strategies, optimal and suboptimal, clearly provide better results than the regular division.

It is also important to notice that, in these simulations, the flights are only performed at certain time instants, and therefore, the performance of the strategy must be evaluated at these points. This fact implies that the evolution of the system after the flight and therefore the initial conditions of the system at the following flights differ. This may provoke that the optimal formulation sometimes performs slightly worse than the heuristic strategy (Algorithm 1). This is due to the fact that the combination of two independently selected optimal paths may become suboptimal in certain situations as the initial conditions for the second flight will be different. However, the

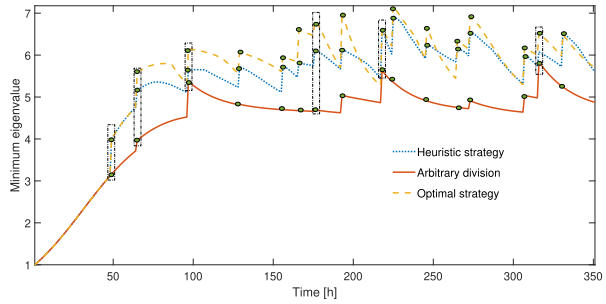

Fig. 10. Evolution of the minimum eigenvalue of the information matrix in a grid of 6×6 nodes. Green dots represent the time instants where a flight was performed.

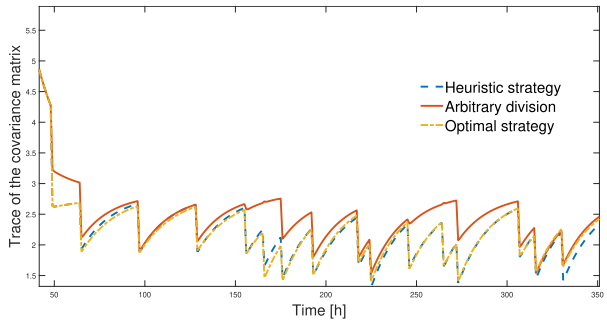

Fig. 11. Evolution of the trace of the covariance matrix in a grid of 6×6 nodes.

results show that this may happen at a very punctual flight and that at all instants, it remains clearly better than the *arbitrary division* approach. In Fig. 10, some of the flight instants are indicated by a rectangle to illustrate the difference in the outcome.

In Fig. 11, the evolution of the trace of the covariance matrix is depicted. It can be seen that the presented strategy also provides much better results at steady state than the usual arbitrary strategy.

Fig. 13 shows the results obtained from a larger scenario, where the area dimensions correspond to a real large-scale hazelnut orchard, as shown in Fig. 12. In this case, the values represented in the plot denote the ratio between the performance of the proposed heuristic strategy and the regular division of the area, which is considered as a lower bound for our performance, and it is computed as

$$R(t) = \frac{\lambda_{1,\text{heur}}(t)}{\lambda_{1,\text{arb}}(t)} \tag{33}$$

where $\lambda_1(t)$ represents the minimum eigenvalue at time k of the Fisher information matrix associated with each strategy. In such a case, $R(t) > 1$ indicates a better performance of the proposed strategy with respect to the regular division.

From Fig. 13, we can observe how the heuristic strategy provides at all instants a better performance than the strategy based only on latency between visits.

Finally, Fig. 14 shows, for a similar field extension and fixed sensors layout, the case where the maximum flying time for the information-based strategy (and only for it) is reduced by 50%. From this plot, it can be seen that even after reducing

Fig. 12. Area considered for the simulation.

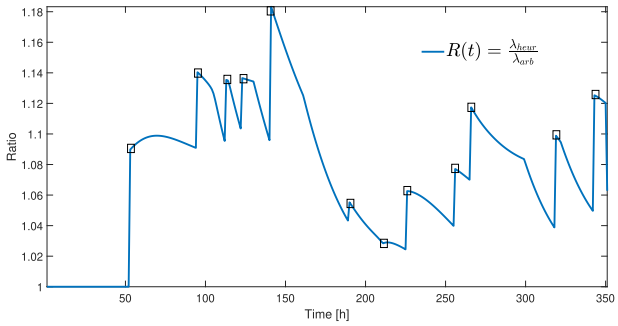

Fig. 13. Ratio between the performances obtained between the strategies. Highlighted by a square the instant related to each flight.

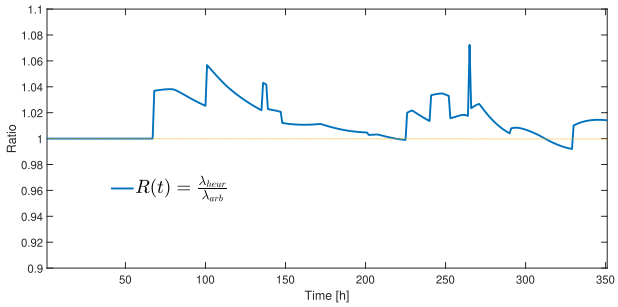

Fig. 14. Evolution of the ratio of performance. Case with reduction of 50% in flying time for the information-based approach (the flight time for the arbitrary division remains the same).

by 50% the flight time, the information-based strategy is still able to obtain really similar results, $R(t) \approx 1$ with $\pm 10\%$, to the regular coverage strategy with the double of the flight time. This result supports one of the main claims of this article, which is that an information-based approach can help to reduce the resources put into the monitoring while keeping a similar performance. This is particularly interesting in the case of UAVs, where the main limiting factor regarding their reduced flight autonomy can be substantially mitigated by this novel strategy.

VII. Conclusion

This article presents a novel path-planning strategy. Focusing on the problem of covering large-scale areas, we propose a path computation strategy where the flying time constraint is

considered and the quality of the estimation of the states of the system is maximized. The problem is formulated as a special OP, which can be written as an MISDP problem. In addition, we present a heuristic with good performance.

The effectiveness of the presented strategy is shown through numerical simulations. These simulations demonstrate a clear improvement in performance with respect to classical strategies. Moreover, the adaptability and flexibility of this approach allow to consider the presence of fixed sensing structures and it is a promising step for the combination with a fleet of mobile robots.

Future works will focus on adapting the presented approach to the case where several vehicles are used. In addition, an important future line of research comprises the definition of new heuristics to solve the presented OP in a more efficient way and/or that provide guarantees of performance with respect to the optimal solution. Other extensions will include the definition of nonmyopic policies for multiple missions with fixed periodicity and the case where the time constants of the monitored system are similar to the flight time of the UAV.

REFERENCES

[1] L. G. Santesteban, S. F. Di Gennaro, A. Herrero-Langreo, C. Miranda, J. B. Royo, and A. Matese, "High-resolution UAV-based thermal imaging to estimate the instantaneous and seasonal variability of plant water status within a vineyard," *Agricult. Water Manage.*, vol. 183, pp. 49–59, Mar. 2017.

[2] K. Themistocleous, A. Agapiou, B. Cuca, and D. G. Hadjimitsis, "Unmanned aerial systems and spectroscopy for remote sensing applications in archaeology," *Int. Arch. Photogramm., Remote Sens. Spatial Inf. Sci.*, vol. XL-7/W3, pp. 1419–1423, Apr. 2015.

[3] Y. Ham, K. K. Han, J. J. Lin, and M. Golparvar-Fard, "Visual monitoring of civil infrastructure systems via camera-equipped unmanned aerial vehicles (UAVs): A review of related works," *Visualizat. Eng.*, vol. 4, no. 1, Dec. 2016.

[4] I. Colomina and P. Molina, "Unmanned aerial systems for photogrammetry and remote sensing: A review," *ISPRS J. Photogramm. Remote Sens.*, vol. 92, pp. 79–97, Jun. 2014.

[5] M. Díaz-Cabrera, J. Cabrera-Gámez, R. Aguasca-Colomo, and K. Miatliuk, "Photogrammetric analysis of images acquired by an UAV," in *Computer Aided Systems Theory—EUROCAST 2013*, R. Moreno-Díaz, F. Pichler, and A. Quesada-Arencibia, Eds. Berlin, Germany: Springer, 2013, pp. 109–116.

[6] S. Alamdari, E. Fata, and S. L. Smith, "Persistent monitoring in discrete environments: Minimizing the maximum weighted latency between observations," *Int. J. Robot. Res.*, vol. 33, no. 1, pp. 138–154, Jan. 2014.

[7] C. G. Cassandras, X. Lin, and X. Ding, "An optimal control approach to the multi-agent persistent monitoring problem," *IEEE Trans. Autom. Control*, vol. 58, no. 4, pp. 947–961, Apr. 2013.

[8] J. Scherer and B. Rinner, "Multi-UAV surveillance with minimum information idleness and latency constraints," *IEEE Robot. Autom. Lett.*, vol. 5, no. 3, pp. 4812–4819, Jul. 2020.

[9] A. T. Klesh, P. T. Kabamba, and A. R. Girard, "Path planning for cooperative time-optimal information collection," in *Proc. Amer. Control Conf.*, Seattle, WA, USA, Jun. 2008, pp. 1991–1996.

[10] K.-C. Ma, Z. Ma, L. Liu, and G. S. Sukhatme, "Multi-robot informative and adaptive planning for persistent environmental monitoring," in *Distributed Autonomous Robotic Systems*, vol. 6, R. Groß, A. Kolling, S. Berman, E. Frazzoli, A. Martinoli, F. Matsuno, and M. Gauci, Eds. Cham, Switzerland: Springer, 2018, pp. 285–298.

[11] V. Suryan and P. Tokekar, "Learning a spatial field in minimum time with a team of robots," *IEEE Trans. Robot.*, vol. 36, no. 5, pp. 1562–1576, Oct. 2020.

[12] R. Cui, Y. Li, and W. Yan, "Mutual information-based multi-AUV path planning for scalar field sampling using multidimensional RRT," *IEEE Trans. Syst., Man, Cybern., Syst.*, vol. 46, no. 7, pp. 993–1004, Jul. 2016.

[13] S. Z. Kang, P. Shi, Y. H. Pan, Z. S. Liang, X. T. Hu, and J. Zhang, "Soil water distribution, uniformity and water-use efficiency under alternate furrow irrigation in arid areas," *Irrigation Sci.*, vol. 19, no. 4, pp. 181–190, Sep. 2000.

[14] T. H. Skaggs, T. J. Trout, and Y. Rothfuss, "Drip irrigation water distribution patterns: Effects of emitter rate, pulsing, and antecedent water," *Soil Sci. Soc. Amer. J.*, vol. 74, no. 6, pp. 1886–1896, 2010.

[15] M. Saidan, A. G. Albaali, E. Alasis, and J. K. Kaldellis, "Experimental study on the effect of dust deposition on solar photovoltaic panels in desert environment," *Renew. Energy*, vol. 92, pp. 499–505, Jul. 2016.

[16] B. Weber, A. Quiñones, R. Almanza, and M. D. Duran, "Performance reduction of PV systems by dust deposition," *Energy Procedia*, vol. 57, pp. 99–108, Jan. 2014.

[17] V. Tzoumas, A. Jadbabaie, and G. J. Pappas, "Sensor placement for optimal Kalman filtering: Fundamental limits, submodularity, and algorithms," in *Proc. Amer. Control Conf. (ACC)*, Jul. 2016, pp. 191–196.

[18] S. Joshi and S. Boyd, "Sensor selection via convex optimization," *IEEE Trans. Signal Process.*, vol. 57, no. 2, pp. 451–462, Feb. 2009.

[19] Y. Mo, E. Garone, A. Casavola, and B. Sinopoli, "Stochastic sensor scheduling for energy constrained estimation in multi-hop wireless sensor networks," *IEEE Trans. Autom. Control*, vol. 56, no. 10, pp. 2489–2495, Oct. 2011.

[20] J. Binney, A. Krause, and G. S. Sukhatme, "Optimizing waypoints for monitoring spatiotemporal phenomena," *Int. J. Robot. Res.*, vol. 32, no. 8, pp. 873–888, Jul. 2013.

[21] S. Garg and N. Ayanian, "Persistent monitoring of stochastic spatio-temporal phenomena with a small team of robots," in *Proc. Robot., Sci. Syst.*, Berkeley, CA, USA, Jul. 2014, pp. 38–47.

[22] X. Lan and M. Schwager, "Planning periodic persistent monitoring trajectories for sensing robots in Gaussian random fields," in *Proc. IEEE Int. Conf. Robot. Autom.*, May 2013, pp. 2415–2420.

[23] B. L. Golden, L. Levy, and R. Vohra, "The orienteering problem," *Nav. Res. Logistics*, vol. 34, no. 3, pp. 307–318, Jun. 1987.

[24] J. Yu, M. Schwager, and D. Rus, "Correlated orienteering problem and its application to persistent monitoring tasks," *IEEE Trans. Robot.*, vol. 32, no. 5, pp. 1106–1118, Oct. 2016.

[25] L. Bottarelli, M. Bicego, J. Blum, and A. Farinelli, "Orienteering-based informative path planning for environmental monitoring," *Eng. Appl. Artif. Intell.*, vol. 77, pp. 46–58, Jan. 2019.

[26] F. Schmidt, H. M. Wainwright, B. Faybishenko, M. Denham, and C. Eddy-Dilek, "*In situ* monitoring of groundwater contamination using the Kalman filter," *Environ. Sci. Technol.*, vol. 52, pp. 7418–7425, Jul. 2018.

[27] J. Fukuda, T. Higuchi, S. Miyazaki, and T. Kato, "A new approach to time-dependent inversion of geodetic data using a Monte Carlo mixture Kalman filter," *Geophys. J. Int.*, vol. 159, no. 1, pp. 17–39, Oct. 2004.

[28] Z. Lin, H. H. T. Liu, and M. Wotton, "Kalman filter-based large-scale wildfire monitoring with a system of UAVs," *IEEE Trans. Ind. Electron.*, vol. 66, no. 1, pp. 606–615, Jan. 2019.

[29] B. Sinopoli, L. Schenato, M. Franceschetti, K. Poolla, M. I. Jordan, and S. S. Sastry, "Kalman filtering with intermittent observations," *IEEE Trans. Autom. Control*, vol. 49, no. 9, pp. 1453–1464, Sep. 2004.

[30] E. Garone, B. Sinopoli, A. Goldsmith, and A. Casavola, "LQG control for MIMO systems over multiple erasure channels with perfect acknowledgment," *IEEE Trans. Autom. Control*, vol. 57, no. 2, pp. 450–456, Feb. 2012.

[31] B. D. O. Anderson and J. B. Moore, *Optimal Filtering*. Englewood Cliffs, NJ, USA: Prentice-Hall, 1979.

[32] M. Segal and E. Weinstein, "A new method for evaluating the log-likelihood gradient, the Hessian, and the Fisher information matrix for linear dynamic systems," *IEEE Trans. Inf. Theory*, vol. 35, no. 3, pp. 682–687, May 1989.

[33] B. Grocholsky, A. Makarenko, and H. Durrant-Whyte, "Information-theoretic coordinated control of multiple sensor platforms," in *Proc. IEEE Int. Conf. Robot. Autom.*, vol. 1, Sep. 2003, pp. 1521–1526.

[34] H. Dette and W. J. Studden, "Geometry of E-optimality," *Ann. Statist.*, vol. 21, no. 1, pp. 416–433, Mar. 1993.

[35] D. Telen, F. Logist, E. Van Derlinden, I. Tack, and J. Van Impe, "Optimal experiment design for dynamic bioprocesses: A multi-objective approach," *Chem. Eng. Sci.*, vol. 78, pp. 82–97, Aug. 2012.

[36] G. Franceschini and S. Macchietto, "Model-based design of experiments for parameter precision: State of the art," *Chem. Eng. Sci.*, vol. 63, no. 19, pp. 4846–4872, Oct. 2008.

[37] C. E. Miller, A. W. Tucker, and R. A. Zemlin, "Integer programming formulation of traveling salesman problems," *J. ACM*, vol. 7, no. 4, pp. 326–329, Oct. 1960.

[38] T. Gally, M. E. Pfetsch, and S. Ulbrich, "A framework for solving mixed-integer semidefinite programs," *Optim. Methods Softw.*, vol. 33, no. 3, pp. 594–632, May 2018.
[39] C. Rowe and J. Maciejowski, "An efficient algorithm for mixed integer semidefinite optimisation," in *Proc. Amer. Control Conf.*, vol. 6, Jun. 2003, pp. 4730–4735.
[40] L. Vandenberghe and S. Boyd, "Semidefinite programming," *SIAM Rev.*, vol. 38, no. 1, pp. 49–95, Mar. 1996.
[41] P. Raghavan and C. D. Tompson, "Randomized rounding: A technique for provably good algorithms and algorithmic proofs," *Combinatorica*, vol. 7, no. 4, pp. 365–374, Dec. 1987.
[42] A. Lipowski and D. Lipowska, "Roulette-wheel selection via stochastic acceptance," *Phys. A, Stat. Mech. Appl.*, vol. 391, no. 6, pp. 2193–2196, Mar. 2012.
[43] F. Yu, X. Fu, H. Li, and G. Dong, "Improved roulette wheel selection-based genetic algorithm for TSP," in *Proc. Int. Conf. Netw. Inf. Syst. Comput. (ICNISC)*, Apr. 2016, pp. 151–154.
[44] N. Bono Rossello, R. Fabrizio Carpio, A. Gasparri, and E. Garone, "A novel observer-based architecture for water management in large-scale (Hazelnut) orchards," *IFAC-PapersOnLine*, vol. 52, no. 30, pp. 62–69, 2019.
[45] J. Jin and L. Tang, "Optimal coverage path planning for arable farming on 2D surfaces," *Trans. ASABE*, vol. 53, no. 1, pp. 283–295, 2010.
[46] M. Coombes, W.-H. Chen, and C. Liu, "Boustrophedon coverage path planning for UAV aerial surveys in wind," in *Proc. Int. Conf. Unmanned Aircr. Syst. (ICUAS)*, Miami, FL, USA, Jun. 2017, pp. 1563–1571.

Nicolas Bono Rossello received the bachelor's and master's degrees in industrial engineering from the Universidad Politècnica de València, València, Spain, in 2017. He is currently pursuing the Ph.D. degree with the Department of Control Engineering and System Analysis, Université Libre De Bruxelles, Brussels, Belgium.

His research interests include path planning and state estimation.

Mr. Bono Rossello received the Young Author Award at the 6th IFAC Agricontrol Conference in 2019.

Renzo Fabrizio Carpio (Graduate Student Member, IEEE) received the bachelor's degree in computer science engineering and master's degree in computer science and automation engineering from Roma Tre University, Rome, Italy, in 2014 and 2017, respectively, where he is currently pursuing the Ph.D. degree in automation and computer science with the Department of Engineering.

In 2018, he worked as a Research Fellow for the project "PANTHEON" focused on robotics for precision farming supported by the European Community within the H2020 framework. His research interests include multirobot control systems, motion and task planning for multirobot systems in outdoor and unstructured environments, and neural networks, mainly in the context of precision farming settings.

Andrea Gasparri (Senior Member, IEEE) received the Laurea degree in computer science *(cum laude)* and the Ph.D. degree in computer science and automation from Roma Tre University, Rome, Italy, in 2004 and 2008, respectively.

He is currently a Professor with the Department of Engineering, Roma Tre University. He is also the Coordinator of the project "PANTHEON" focused on robotics for precision farming supported by the European Community within the H2020 framework and the project "CANOPIES" focused on the development of a collaborative paradigm for human workers and multirobot teams in precision agriculture systems within the H2020 framework. His research interests are in the areas of robotics, sensor networks, networked multiagent systems, and precision agriculture.

Dr. Gasparri has been a member of the Steering Committee of the IEEE RAS Technical Committee on Multirobot Systems since 2014 and the IEEE CSS Technical Committee on Networks and Communications since 2015. He received the Italian Grant FIRB Futuro in Ricerca 2008 for the project Networked Collaborative Team of Autonomous Robots funded by the Italian Ministry of Research and Education. He has been an Associate Editor of the IEEE TRANSACTIONS ON CONTROL OF NETWORK SYSTEMS since 2021. He was an Associate Editor of the IEEE TRANSACTIONS ON CYBERNETICS from 2017 to 2020.

Emanuele Garone received the master's degree (Laurea) and the Ph.D. degree in systems engineering from the University of Calabria, Rende, Italy, in 2005 and 2009, respectively.

Since 2010, he has been an Associate Professor with the Department of Control Design and System Analysis, Université Libre de Bruxelles, Brussels, Belgium. He has authored more than 160 contributions in peer-reviewed conferences and journals. His research interests include constrained control, reference governors, networked control systems, and aerial robotics.

Dr. Garone received the Honorable Mention for the Young Author Prize of the 19th IFAC World Congress in 2014.